

Theoretical Investigation of the Anion Binding Affinities of the Uranyl Salophene Complexes

Marcin Brynda,^{*,†} Tomasz A. Wesolowski,^{‡,||} and Kamil Wojciechowski^{§,⊥}

Department of Chemistry, University of California, Davis, One Shields Avenue, Davis, California 95616, Department of Physical Chemistry, University of Geneva, 30 Quai Ernest Ansermet, 1211 Geneva 4, Switzerland, and Department of Analytical, Inorganic and Applied Chemistry, University of Geneva, 30 Quai Ernest Ansermet, 1211 Geneva 4, Switzerland

Received: February 9, 2004; In Final Form: March 16, 2004

The uranyl salophene complex and its co-complexes with several anions (H_2PO_4^- , HSO_4^- , NO_2^- , OH^- , Cl^- , F^-) in the gas phase are investigated theoretically. Equilibrium geometries of relevant species and complexation-induced structural changes are discussed. The ^{13}C NMR chemical shifts calculated at the gas-phase optimized geometry agree very well with experimental liquid-phase results. The optimized geometry agrees also very well with available crystallographic data. This indicates that the gas-phase structures derived from theoretical calculations can be considered representative also for the condensed phase. For all anions, except H_2PO_4^- , the calculated gas-phase binding energies correlate well with experimental Gibbs free energies of complexation. The possible role of the solvent in the case of H_2PO_4^- complexation is discussed.

Introduction

The increasing need for the nuclear waste complexants in the last two decades led to the extensive search of molecules capable of specifically binding radioactive ions in order to separate them from others. Uranium(VI) in its stable uranyl form (UO_2^{2+}) is especially interesting due to its high affinity for some environmentally relevant carbonate, phosphate, or hydroxide ions. The phosphate ions, important components of many fertilizers, form very poorly soluble salts with UO_2^{2+} .¹ The affinity of phosphates to a uranyl ion is so high that most of the phosphate-containing fertilizers contain significant amounts of uranium.²

The high affinity of phosphate ions to UO_2^{2+} can also be used for analytical purposes, e.g., to determine the phosphate concentration in water. The environmental importance of phosphate ions contrasts with a rather limited number of available analytical methods suitable for their determination. So far, the analytical chemistry of the phosphate ions relies mostly on their ability to form a heteropoly complex with molybdenic acid, which can be determined spectrophotometrically. In principle, the high selectivity of phosphate ion recognition by uranyl ion could be used for analytical purposes. Very strong binding of bare UO_2^{2+} to anions such as H_2PO_4^- or F^- ^{36a} prevents it, however, from being used as a *host* in that form for the recognition of anions. To be useful in molecular recognition, the complexation of a *guest* (target anion) by the *host* (UO_2^{2+}) should not be too strong. For example, Izatt et al. found that the maximum efficiency of the alkali and alkaline earth metal ions transport by the crown ethers through the nonpolar phase is attained when the complex stability in

methanol is in the 10^5 – 10^7 M^{-1} range.³ The convenient way to modify the complexing properties of a metal ion is its immobilization in the cavity of an organic ligand. In most complexes, the coordination sphere of UO_2^{2+} is pentagonal or hexagonal, with few exceptions showing different geometry, such as in the highly constrained systems, homooxacalixarenes.⁴ The unique coordination geometry of the uranyl ion makes it possible to build even the three-dimensional cage-like structures with Kemp's triacid.⁵ An uranyl cation is complexed by a number of "uranophiles", like the complexing agents containing diaza bonds: PAN (phenyl-azo-2-naphthol), Arsenazo (7-hydroxy-8-(phenylazo)-1,3-naphthalenedisulfonic acid), as well as by macrocyclic ligands: calixarenes and crown ethers.⁶ None of them, however, provides the complex geometry suitable for co-complexation of the second ligand (target anion), since all the equatorial positions are occupied by the donor atoms of these "uranophiles".

Bandoli and Clemente⁷ were the first who reported the complexes of the Schiff base with uranyl, possessing one free equatorial coordinating position, usually occupied by a weakly bound solvent molecule. For this purpose, N_2O_2 -type ligands derived from the product of salicylaldehyde and diamines condensation (see Figure 1a) were used. According to the commonly used nomenclature, the product of an aliphatic amine condensation is called salene, and that of an aromatic amine condensation is called salophene. In sal(oph)ene complexes, U(VI) ion is seven-coordinated, with two oxygen atoms in axial positions and five other coordinating positions located in the equatorial plane (pentagonal bipyramid). Anchoring UO_2^{2+} inside the sal(oph)ene moiety blocks four out of five equatorial positions in the coordination sphere of UO_2^{2+} (see Figure 1b). In the early nineties, Reinhoudt et al. showed the first few examples where the solvent occupying the fifth equatorial position was replaced by other, electron-rich molecules, such as urea, formamide,⁸ or anions.⁹

The planar structure of the sal(oph)ene-type Schiff bases is especially suited for the bipyramidal pentagonal geometry of

* Corresponding author. E-mail: mabrynda@ucdavis.edu.

† Department of Chemistry, University of California Davis.

‡ Department of Physical Chemistry, University of Geneva.

§ Department of Analytical, Inorganic and Applied Chemistry, University of Geneva.

|| E-mail: tomasz.wesolowski@chiphpy.unige.ch.

⊥ E-mail: kamil.wojciechowski@cabe.unige.ch.

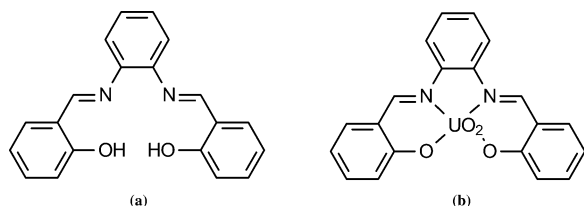


Figure 1. The chemical structure of the salophene (a) and its uranyl complex: uranyl salophene **US1** (b).

TABLE 1: The Experimental Stability Constants (K_{ass}) and Corresponding Gibbs Free Energies (ΔG) for the Uranyl Salophene (US1**) Complexation with Anions Determined Conductometrically in a Mixture Acetonitrile/DMSO (99:1)^a**

complex	K_{ass} [M^{-1}]	ΔG [kcal mol ⁻¹]
Sal- UO_2 - Cl^-	4.5×10^2	-15.2
Sal- UO_2 - NO_2^-	3.1×10^2	-14.2
Sal- UO_2 - HSO_4^-	5.0×10^1	-9.7
Sal- UO_2 - H_2PO_4^-	1.1×10^4	-23.1

^a Adapted from ref 27.

the uranyl ion, which fits well in their semi-cavity, to form stable electroneutral complexes. The presence of two or three aromatic rings renders the sal(oph)ene structure relatively versatile. By using the appropriate derivatives of salicylaldehyde and/or diamines, one can influence both electronic and sterical properties of the uranyl center, thus fine-tuning the active center to the suited *guest* (anion). The effect of different substituents on the selectivity of anion recognition was extensively studied.¹⁰ For example, the presence of hydrogen-bond donors in the proximity of the uranyl center significantly improves the affinity of such a receptor to the fluoride anion.¹¹

Reinhoudt et al. found that uranyl salophenes can selectively bind H_2PO_4^- , F^- , and OH^- ions in organic solution and in the polymeric membrane of the ISEs (ion selective electrodes).^{9,25} As expected, due to the high affinity of UO_2^{2+} to phosphate anions,²⁶ the stability constants in the solution for a series of complexes of the simple salophenes with these anions are larger than those of Cl^- , NO_2^- , and even HSO_4^- complexes (see Table 1). A much weaker binding of the latter ion is surprising, since phosphate and sulfate geometrical and electronic structures are similar. Further research on the anion recognition by uranyl salophenes showed that the prolonged contact of the latter with the solution containing the phosphate ions results in decomposition of the ionophore.²⁸ This observation suggests that the anion binding by uranyl salophenes in the case of H_2PO_4^- is of a special nature; the presence of any other ion did not result in the formation of such stable complex, nor in the ionophore degradation.

Despite the extensive research in the domain of anion recognition by uranyl sal(oph)enes, the determination of the complex structure was possible only for few uranyl salophene-anion complexes.^{7-9,17g,32} The computational chemistry can supply in these cases supplementary information on the geometries and binding energies of the complexes, which are otherwise difficult to determine. To our knowledge, the only theoretical studies on uranyl salophenes were performed with molecular mechanics QUANTA/CHARM, more than a decade ago.^{8,17f} In these studies, only the complexes with neutral molecules using a point charge model for UO_2^{2+} were investigated.

The quantum chemistry investigations of uranium-containing molecules were carried out over the last 20 years. Only recently, the methods enabling the researchers the accurate calculations of UO_2^{2+} complexes became available. Most of the work

published focuses on the quantum mechanics geometry optimization of the small molecules containing uranium.¹⁴ Another group of literature data deals with the complexation of a uranyl ion by water molecules.¹⁵ Early attempts to use quantum mechanical methods for the optimization of the geometry of the small molecules containing uranium gave a realistic bond length for the free uranyl ion in the range of 1.66–1.70 Å¹⁵ calculated at a Hartree–Fock (HF) level with quasirelativistic pseudopotential. Interestingly, as opposed to the large amount of available experimental data, there is only a limited amount of theoretical works on the binding affinities of the UO_2^{2+} . Craw et al. reported the geometry optimizations of the UO_2^{2+} complexes with nitrates and sulfates, performed at the Restricted Hartree–Fock (RHF) level^{17a} and found that the complexation of these anions is of a mainly electrostatic nature. Stronger binding of sulfate ions, as compared to nitrates, was attributed to the charge-transfer contribution to the binding energy. Wipff and collaborators studied monomeric and dimeric complexes of UO_2^{2+} with Ph_3PO , Me_3PO , and NO_3^- ,^{17b} and also stressed the importance of charge transfer and polarization effects. The latter were proposed to be the origin of increased affinity of uranyl to aromatic phosphine oxides. The electronic reorganization resulting from the anion binding was shown to influence significantly the solvation free energies and thus the selectivity of recognition in the solution for phosphine oxide ligands. Recently, Wipff et al. reported a computational study^{17c} at a HF level in which the calculated binding affinities (perchlorate < triflate < nitrate) were confirmed by the EXAFS investigations on the affinity of the perchlorate and triflate ions to UO_2^{2+} . In the report by Reich et al. on uranyl carbonates^{17d} and their complexes with Ca^{2+} and Ba^{2+} , the authors noticed that the U–O distances obtained in the case of the $\text{UO}_2(\text{CO}_3)_3^{4-}$ complexes were too long if the solvent effects were not explicitly taken into account. The uranyl carbonate was also investigated by Nitsche et al.,^{17e} who successively reproduced its vibrational frequencies using Density Functional Theory (DFT) calculations. A review of computational methods applied in the studies of complexation properties of uranium, which includes the DFT calculations, was published by Pepper¹² and more recently by Kaltsoyannis.¹³

The aim of this work was to get additional insight into the nature of the complexation of selected anions to the uranyl salophene. The ultimate goal of our research is the understanding of high selectivity of recognition of H_2PO_4^- ions in the condensed phase. No studies were performed so far on the origin of this selectivity. This work presents the first approach to the problem, the study of anion binding properties of uranyl salophene **US1** in the gas phase. Besides H_2PO_4^- we selected other strongly (OH^- , F^-) and weakly (Cl^- , NO_2^- , HSO_4^-) bound anions in order to compare the mode of anion bonding in the complex with **US1**, and to validate the binding energy calculations. The calculated gas-phase affinities were compared with these observed in solution to estimate the importance of solvent effects on the condensed-phase binding energies. The understanding of the origin of phosphate recognition selectivity in the condensed phase could help to design better uranyl sal(oph)ene-based hosts for these ions. Thus, more selective sensors could be designed and hopefully applied in the environmental analysis.

Computational Methods

The quantum mechanical investigation of uranyl salophenes is a computationally expensive task. For this reason we decided to use DFT, which is known to accurately reproduce the

structure and thermochemistry of uranium(VI) complexes.¹⁸ In most of the studies described in the literature, a description of the core electrons of the uranium atom with quasirelativistic pseudopotential was combined with the use of hybrid functionals. In this method, the effects of the core electrons on valence shell is represented by the Effective Core Potential (ECP), which significantly reduces the computational costs while taking into account the relativistic effects. Adamo et al., however, pointed out that the use of such an approach in the investigation of heavy elements such as uranium may sometimes lead to erroneous results.¹⁸ Nevertheless, dedicated studies for uranyl complexes showed that the experimental data, the ECP results, and the ones obtained from the Zero Order Relativistic Approximation (ZORA) relativistic Hamiltonian, which treats the core electrons explicitly, are in satisfactory agreement.^{37b}

For the geometry optimization we used the ADF program²⁰ in which the ZORA Hamiltonian is combined with Kohn–Sham formalism using Becke^{20c}–Perdew^{20d} approximation to the exchange–correlation functional and Slater Type of Orbitals of triple- ζ quality (basis IV). Throughout the text, this implementation is labeled as KS(ZORA).

For comparison purposes, some properties were calculated also using the quasirelativistic pseudopotential approach with the nonrelativistic Hamiltonian, as implemented in the Gaussian 03 package.²¹ The Wood-Boring Stuttgart/Dresden relativistic large core ECP basis set (ECP78MWB–78 electrons in the core (8s,8p,6d,5f,2g) \rightarrow (5s,5p,4d,3f,2g) contracted-valence basis set)^{24a,b} for uranium and 6-31 g* basis sets for all the other atoms were used. The B3LYP^{24c} approximation to the exchange–correlation functional was used. This second implementation is labeled as KS(ECP) throughout the text.

The KS(ZORA) implementation was used to derive (a) the optimized geometry of salophene, uranyl salophene complex (**US1**), and its co-complexes with anions, (b) binding energies, and (c) Mulliken charges. The KS(ECP) implementation was used to derive (a) binding energies, (b) ¹³C NMR chemical shifts calculated using the GIAO (Gauge Independent Atomic Orbital) method, as implemented in the Gaussian 03 package;²¹ for this particular purpose we used several basis sets of increasing quality (3-21g*, 6-31g*, 6-31+g* and 6-31++g**), (c) the atomic orbitals (AO) contributions to molecular orbitals (MOs) and overlap populations calculated using the AOMix program,²³ (d) optimized geometry of the Mg²⁺–salophene complex for some auxiliary analysis.

The binding energies discussed in the text were corrected for Basis Set Superposition Error (BSSE) using the counterpoise method of Boys and Bernardi.^{24d}

Results and Discussion

Uranyl Salophene Complex (US1). In the first stage of the study, the geometry of the neutral (protonated) salophene molecule was optimized (Figure 1a). Despite the presence of three aromatic rings, connected by the imine bonds, the protonated salophene is not planar in its energy minimum. The two rings containing phenolic groups are tilted, probably due to repelling of the phenolic OH groups. The rotation around the C(aromatic)–N bond is relatively free and the calculated energy barrier of rotation²⁹ equals 2.6 kcal mol⁻¹. The very small difference in energy calculated for the two lowest energy isomers ($\Delta E = 0.05$ kcal mol⁻¹) suggests that both rotamers should coexist in the gas phase (see Supporting Information).

The optimized structure of the free salophene was used to construct the starting geometry of **US1**, in which the UO₂²⁺ was located in the cavity of the salophene. Due to the

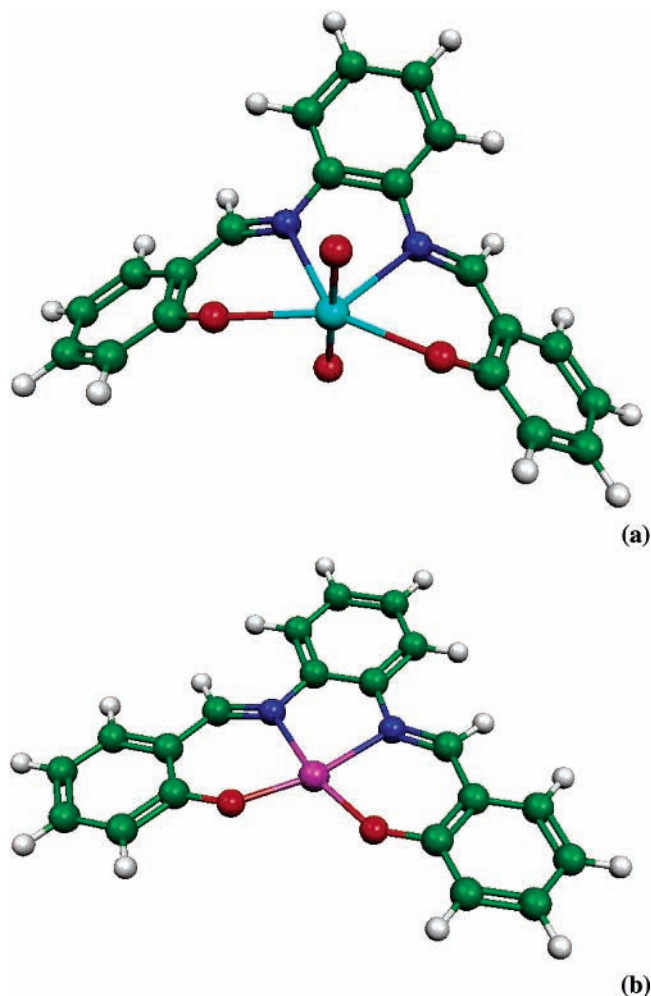


Figure 2. The optimized structures of complexes of salophene with: UO₂²⁺ (a), and Mg²⁺ (b).

deprotonation of the salophene ligand, the complex of uranyl ion with salophene (uranyl salophene, **US1**) is electrically neutral. The ionic radius of the uranyl ion (2.80 Å) is slightly bigger than the radius of the semi-cavity of the salophene moiety. Despite this mismatch, the negative charge of two phenolic groups and the presence of the free electron pairs on two imine nitrogens drive the ion into the semi-cavity. Its incorporation requires, however, slight “puckering” of the Schiff base, leading to a bent structure of **US1** (U–O_{equatorial}–C_{aromatic} angle equals 137.6°).

To confirm the steric origin of the “puckering” of the salophene moiety, the geometry of the complex with the Mg²⁺ cation, which is less sterically demanding (ionic radius 0.72 Å compared to 2.80 Å for UO₂²⁺), was optimized. The structures of both complexes are shown in Figure 2. The presence of the Mg²⁺ ion in the semi-cavity results in an almost ideally flat structure, with all three aromatic rings lying in the same plane, which confirms our interpretation of the origin of the salophene bending upon binding UO₂²⁺.

Recently, Mandolini et al.³⁰ showed that the uranyl salophenes exist as a pair of enantiomers due to slight “puckering” of the whole molecule. At room temperature, in the absence of any steric hindrances, the rate of the interconversion is so high that the presence of two enantiomers is not detected by the NMR technique. Our calculations confirm that uranyl salophenes may indeed exist as a pair of enantiomers, due to the tilt of the two aromatic rings with respect to the equatorial plane of UO₂²⁺.

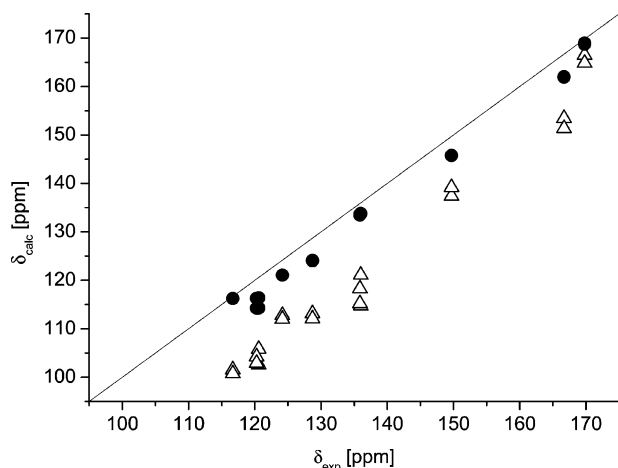


Figure 3. Correlation between experimental and calculated ^{13}C chemical shifts for **US1**: the gas-phase optimized (\bullet) and X-ray structure (Δ). The solid line represents the ideal correlation between two sets of chemical shifts.

The calculated uranyl salophene geometry could not be directly compared with experimental data, due to lack of the corresponding X-ray structure. Nevertheless, the calculated bond lengths (2.255, 2.530, and 1.808 Å for U–O(Ph), U–N, and U=O, respectively) are very close to the values for the aqua-complexes of similar compound (two $-\text{OCH}_3$ substituents in the positions *ortho* vs the phenolic groups): 2.41, 2.53, and 1.77 Å for U–O(Ph), U–N, and U=O, respectively.

The additional support for the relevance of the calculated structures comes from the analysis of the carbon shielding tensors³¹ which are known to depend strongly on the geometry of a molecule. The calculated ^{13}C NMR chemical shifts corresponding to the optimized structure were compared with the experimental data in $\text{DMSO}-d_6$ solution. The details concerning the assignment of the carbon atoms in **US1** can be found in the Supporting Information. The correlation between the calculated chemical shifts and those obtained from experiment is shown in Figure 3. For comparison, the chemical shifts were also calculated for the **US1** structure taken from X-ray of **US1-Cl**.^{9b} The calculated chemical shifts obtained from the gas-phase calculations depend strongly on the chosen basis set and geometry. The use of the extended basis set (6-31++g**) on the KS(ZORA)-optimized geometry results in very good agreement with the experimental data from the solution NMR spectrum. For the nonoptimized geometry and/or the basis set of insufficient quality, the chemical shifts correlate much worse with the experimental points. Data obtained from the X-ray structure using the 6-31++g** basis set is shown for comparison in Figure 3. The X-ray structure, despite its overall resemblance to the gas-phase optimized structure, gives rise to the chemical shifts of some carbon nuclei lying outside the expected range in the NMR spectrum. As indicated by the analysis of the calculated ^{13}C chemical shifts, the gas-phase optimized structure is probably closer to that in solution than is the X-ray structure.

The energy of UO_2^{2+} complexation inside the semi-cavity of salophene was calculated at the optimized structure of **US1** using the KS(ECP) method. The enthalpy of the reaction of the doubly deprotonated salophene anion with UO_2^{2+} is equal to $-820.1 \text{ kcal mol}^{-1}$. Such high enthalpy of uranyl binding stabilizes the uranyl ion in the salophene complex, which justifies the use of uranyl salophenes for the purposes of molecular recognition.

TABLE 2: Selected Geometrical Parameters of the DFT Optimized Structures

species	U=O	U–O	U–N	U–Ion	$\angle\text{OUO}$
UO_2^{2+}	1.722				180.0
Sal- UO_2	1.808	2.255	2.530		179.6
Sal- $\text{UO}_2\text{-Cl}^-$	1.815	2.315	2.716	2.686	172.5
Sal- $\text{UO}_2\text{-F}^-$	1.822	2.348	2.708	2.142	172.4
Sal- $\text{UO}_2\text{-OH}^-$	1.825	2.362	2.746	2.187	175.9
Sal- $\text{UO}_2\text{-NO}_2^-$	1.815	2.313	2.690	2.347	174.8
Sal- $\text{UO}_2\text{-HSO}_4^-$	1.816	2.218	2.676	2.421	174.5
Sal- $\text{UO}_2\text{-H}_2\text{PO}_4^-$	1.813	2.310	2.692	2.326	173.6

TABLE 3: The Calculated Binding Energies (kcal mol^{-1}) of the US1–Anion Complexes in the Gas Phase^a

complex	$\Delta E_{\text{KS(ZORA)}}$	$\Delta E_{\text{KS(ECP)}}$
Sal- $\text{UO}_2\text{-HSO}_4^-$	-21.5	-23.1
Sal- $\text{UO}_2\text{-Cl}^-$	-40.2	-35.4
Sal- $\text{UO}_2\text{-H}_2\text{PO}_4^-$	-35.3	-36.8
Sal- $\text{UO}_2\text{-NO}_2^-$	-35.2	-37.7
Sal- $\text{UO}_2\text{-F}^-$	-72.6	-70.3
Sal- $\text{UO}_2\text{-OH}^-$	-70.3	-70.6

^a For the description of the applied methods see the Experimental Section.

TABLE 4: The Calculated Energies (ΔE) of Substitution of Salophene Moiety by the Anion in the US1–Anion Complexes (kcal mol^{-1})

complexed anion (X^-)	F^-	OH^-	H_2PO_4^-	Cl^-
ΔE	+47.2	+46.1	+113.2	+146.9

TABLE 5: Charge Distribution for the Selected Atoms in the Anionic Complexes of US1 Optimized

species	U	O(UO_2)	O(Ph)	N	anion
UO_2^{2+}	2.08	-0.04			
Sal- H_2			-0.66	-0.60	
Sal- UO_2	1.25	-0.34	-0.58	-0.50	
Sal- $\text{UO}_2\text{-Cl}^-$	1.06	-0.36	-0.56	-0.46	-0.43
Sal- $\text{UO}_2\text{-F}^-$	1.10	-0.37	-0.56	-0.46	-0.38
Sal- $\text{UO}_2\text{-OH}^-$	1.08	-0.38	-0.56	-0.46	-0.31
Sal- $\text{UO}_2\text{-NO}_2^-$	1.16	-0.36	-0.56	-0.46	-0.56
Sal- $\text{UO}_2\text{-HSO}_4^-$	1.17	-0.36	-0.57	-0.47	-0.64
Sal- $\text{UO}_2\text{-H}_2\text{PO}_4^-$	1.18	-0.35	-0.56	-0.47	-0.59

Uranyl Salophene Complexes with Anions. Due to the high affinity of the uranyl ion to some hard anions, such as F^- or H_2PO_4^- , one can expect that binding of these anions could induce changes in the uranyl salophene geometry. In the next stage of the present study, the structural changes accompanying the anion complexation were investigated. The key geometrical parameters of the gas-phase optimized structures are reported in Table 2. The uranyl moiety elongates upon complexation with a salophene anion by 0.005–0.017 Å, most probably due to partial compensation of positive charge on the U atom by the salophene (see Table 5). The overall shape of the uranyl salophene is not significantly affected by the complexation of the anions. **US1** might be considered as a well pre-organized *host* for the studied anions. The complexation of the anions does not require any significant structural rearrangement of **US1**, which could involve unfavorable entropy changes. The optimized structures of the anionic complexes are shown in Figure 4.

The only experimental values of the UO_2^{2+} –anion distance in the uranyl salophene–anion complexes available in the literature (2.76 and 2.28 Å, for Cl^- and H_2PO_4^- , respectively) are close to those obtained from our calculations (2.686 Å, 2.326 Å). These small discrepancies might stem from the crystal packing forces and the fact that the solid-state stoichiometry might be different from that in the gas phase. The X-ray

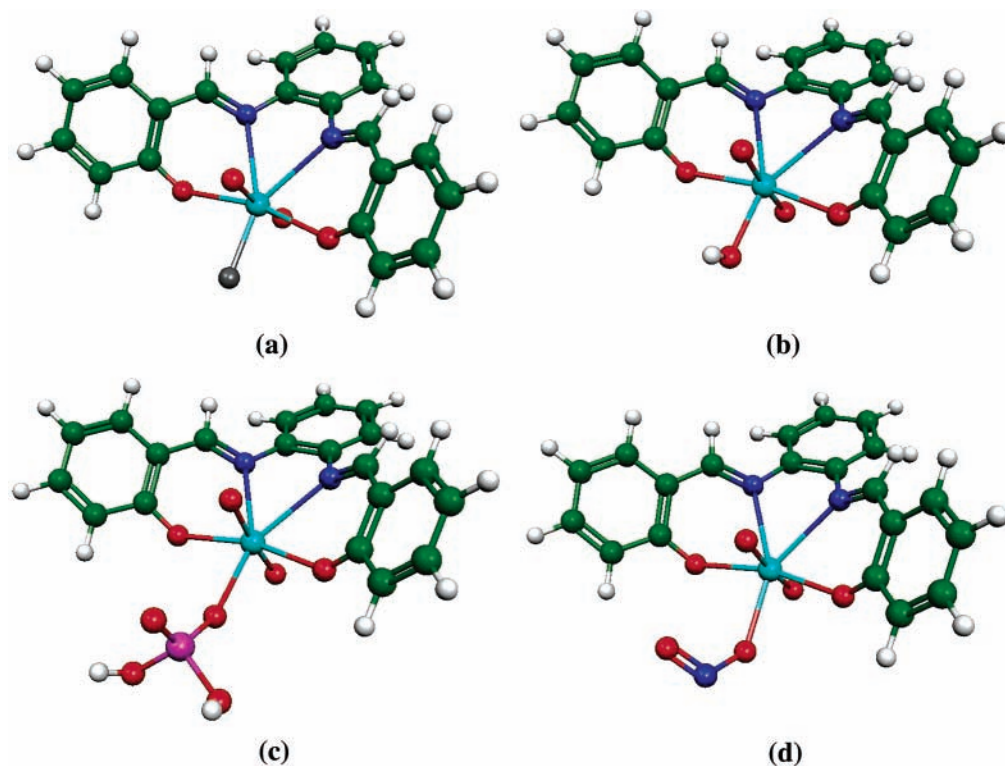


Figure 4. The optimized structures of the selected anionic complexes of **US1**. Calculations performed for: **US1**– F^- (a), **US1**– OH^- (b), **US1**– H_2PO_4^- (c), **US1**– NO_2^- (d).

structure⁹ of the uranyl salophene– H_2PO_4^- complex (see Supporting Information), which is a centro-symmetric dimer, indicates that the stoichiometry of the complex is 2:2 rather than 1:1. Moreover, the existence of a similar structure in nonpolar solvents, although with 2:1 stoichiometry, was reported.³²

We start the analysis of the complexation-induced geometrical changes of **US1** from the uranyl moiety. The $\text{U}=\text{O}$ bond in the uranyl as well as the $\text{U}-\text{O}$ distance between the uranium atom and the phenolic oxygen atom elongate in the **US1**–anion complexes. This effect is the most pronounced in the F^- and OH^- complexes, where the uranyl $\text{U}=\text{O}$ bond length elongates from 1.808 to 1.822 Å and 1.825 Å, respectively. Similar trends were observed in the case of coordination of anions to *bare* UO_2^{2+} . The $\text{U}=\text{O}$ distance increases from 1.71 to 1.74 Å when ClO_4^- is replaced by the CH_3COO^- ion.^{36b,c} These trends are also consistent with the ones observed by Marsden et al.³³ who found a strong correlation between the binding energy of the ligand and the length of the $\text{U}=\text{O}$ bond in the UO_2^{2+} ion. In their study, the largest change (0.084 Å) was found for $\text{UO}_2(\text{OH})_2$. The bond elongation is more pronounced than in the case of the **US1** complex (0.017 Å), but the two numbers correspond to binding of different numbers of OH^- ions to two different species (free uranyl ion, and uranyl salophene, respectively). Our results concern UO_2^{2+} incorporated in the cavity of salophene moiety, where only one OH^- can be complexed. In addition, the charge on the U atom is significantly smaller than in the free uranyl ion, as indicated by the Mulliken population analysis (1.25e in **US1** and 2.08e in UO_2^{2+}). In the case of the weakly bound anions (Cl^- , NO_2^- , HSO_4^- , H_2PO_4^- ; see Table 3), the changes in the axial oxygen distance do not exceed 0.008 Å (see Table 2). Similarly, only small changes in the $\text{U}=\text{O}$ distance were observed in the X-ray structures³⁴ if the fifth equatorial coordination position of uranyl salophene is occupied by the weakly coordinating solvent.

In the anionic complexes, the $\text{O}=\text{U}=\text{O}$ moiety is not linear. The $\text{O}=\text{U}=\text{O}$ angle falls in the range from 172.4° to 175.9°, depending on the anion (see Table 2). A similar bending of the linear UO_2^{2+} moiety upon complexation with OH^- ions was reported for the calculated gas-phase complexes by Tsushima and Reich,³⁵ who interpreted this in terms of π -donation from the equatorial hydroxyl ion. Similar nonsymmetrical donation from the equatorially anions to salophene-bound uranyl could result in the observed deviation from $\text{O}=\text{U}=\text{O}$ linearity. The effect of the presence of an equatorially complexed *guest* anion cannot be compensated by the complexation of the ion of the same type in trans position in uranyl salophene for steric reasons.

The $\text{U}-\text{O}(\text{phenolic})$ bond elongation is also noticeable. The bond length increases from 2.255 to 2.348 Å and 2.362 Å for F^- and OH^- complexes, respectively. The distance between the U and N atoms is also affected. As in the case of the $\text{U}-\text{O}$ distance, the most pronounced effect can be seen for F^- and OH^- complexes. For these two complexes, the $\text{U}-\text{N}$ distance changes from 2.530 to 2.708 Å and 2.746 Å, respectively. There is also a small, but noticeable, change in the geometry of the uranyl center. The elongation of the $\text{U}-\text{O}$ and $\text{U}-\text{N}$ bonds is probably related to the increase of the electron density on the U atom, as shown by the Mulliken analysis (see Table 5). As a result of the increase of the $\text{U}-\text{O}(\text{phenolic})$ and $\text{U}-\text{N}(\text{imine})$ distances, the size of the semi-cavity of **US1** increases to accommodate the complexed anion.

The binding energies were calculated using the following convention:

$$\Delta E = E[\text{US1}-\text{X}^-] - E[\text{US1}] - E[\text{X}^-]$$

The results of calculations using KS(ZORA) and KS(ECP) methods are collected in Table 3. The comparison of the two sets of data shows that both methods give similar results. The

relative difference between the binding energies calculated using the two approaches does not exceed 10% for the complexes with these anions.

As can be seen in Table 3, the interaction energy decreases in the following order: $F^- > OH^- > Cl^- > H_2PO_4^- > NO_2^- > HSO_4^-$. According to our expectations, the relative order of the gas-phase binding energies is (with the exception of $H_2PO_4^-$, see below) similar to the order observed experimentally for complexes of **US1** in solution (Table 1), as well as with general trends in binding affinity of UO_2^{2+} to anions.^{36a}

To our knowledge, no studies on thermodynamics of binding of F^- or OH^- ions to **US1** were reported in the literature. Some indirect information on the affinity of these ions to uranyl sal(oph)enes can be deduced, however, from the potentiometric selectivity of the sensors containing uranyl salophenes as the ionophore. Despite high hydrophilicity of phosphate and fluoride ions, the sensors containing uranyl sal(oph)enes show an increased selectivity toward these ions, suggesting that they are selectively complexed by uranyl salophenes. On the other hand, an interference of OH^- on $H_2PO_4^-$ and F^- response was observed during potentiometric measurements with uranyl salophenes as ionophores in the phosphate selective electrodes,²⁵ suggesting that also OH^- ions can compete with the strongly complexed $H_2PO_4^-$ ion (see Table 1).

The formation of hydroxo-bridges was shown to play a key role in the speciation of uranyl in natural waters.^{37a} Bruno et al. pointed out the crucial role played by these bridges in the stability of polynuclear uranyl complexes.^{37b} Even though the formation of any oligomeric structures was not considered in this study, the results show an increased affinity of **US1** to OH^- . One might expect that this affinity should be even higher in solution, due to the stabilizing solvent effects, but the complexation of OH^- remains out of the scope of this work.

On the basis of their *ab initio* calculations, Thatcher et al.³⁸ pointed out the important role of the stereochemistry of hydrogen bonding in the selectivity of recognition of sulfate and phosphate ions by the natural receptor binding sites. On the basis of our calculations, the geometries of the **US1**– $H_2PO_4^-$ and **US1**– HSO_4^- complexes do not differ significantly. For the **US1**–anion complexes, the directionality of anion binding plays, however, a less important role than in the hydrogen-bonded complexes.

Marsden et al.³³ in their DFT study of 33 uranyl complexes with small ligands also found the binding energy for OH^- and F^- complexes to be the highest in the whole data set. This is in agreement with the present results for the complexation of these ions to **US1** (see Table 3). Unfortunately, the complexes with phosphate anions were not included in the study of Marsden et al.

As mentioned in the Introduction, the high affinity of phosphate ions to the uranyl salophenes results in the deactivation of the latter: the ion-selective electrodes with membranes containing uranyl salophenes as ionophores lose their phosphate selectivity after prolonged exposure to the phosphate solution. There is no experimental data concerning this phenomenon in the gas phase. Such a process can be accounted for, however, by calculating the enthalpy of the hypothetical reaction leading to uranyl salophene decomposition. The following two-step decomposition pathway of uranyl sal(oph)enes by the phosphate ions in the presence of water was proposed on the basis of the spectroscopic data:²⁸

(1) the uranyl salophene dissociates and hardly soluble uranyl phosphate is formed, due to the high affinity of phosphates to free uranyl ion,

(2) phosphate ions hydrolyze the liberated salophene (acid hydrolysis of the Schiff base).

The enthalpic contribution to such a process can be calculated as the enthalpy of the first reaction, i.e., the substitution of salophene in the **US1**–anion complex by the second anion of the same type (X^-). The enthalpy of such a process was calculated using the following convention:

$$\Delta E = E[UO_2(\text{salophene})-(X^-)] + E[X^-] - E[UO_2(X)_2] - E[\text{salophene}^{2-}]$$

The calculated energies of such a substitution reaction for four ions under study show that phosphate ions, similarly to others, are not able to substitute the salophene moiety in the ternary complex (Table 4). In all cases the energy is positive, in agreement with experimentally observed high kinetic stability of uranyl salophenes in the presence of studied anions (except for $H_2PO_4^-$). Interestingly, the substitution energy for the **US1**– $H_2PO_4^-$ complex is similar to that of the **US1**– Cl^- complex, despite a big difference in their kinetic stability. The decomposition of **US1** in the presence of phosphate ions is then probably related to the specific interaction between the molecules in solutions, which are not taken into account in our gas-phase calculations (see below).

Phosphate-Ion Complexation. The gas-phase interaction energy correlates well with the available experimental free Gibbs energy of complexation in the anhydrous acetonitrile/DMSO (99/1, v/v) mixture for the HSO_4^- , NO_2^- , or Cl^- complexes. Opposite to our expectations, the energy of $H_2PO_4^-$ complexation by **US1** in the gas phase is comparable to those of HSO_4^- , NO_2^- , or Cl^- , despite the exceptionally strong complexation of the dihydrogenphosphate ion observed in the anhydrous acetonitrile/DMSO (99/1, v/v) mixture (see Table 1). The high selectivity of phosphate binding by **US1** in the solution cannot be thus explained only in terms of the gas-phase binding energies. The interactions with the solvent influence all the relevant thermodynamic states in the solution: free anions, **US1**, and its anionic complexes. Since the solvation of **US1** does not depend on the type of the complex, the observed difference might only stem from the differences in the solvation of the free ions and their **US1**-complexes. In our opinion the exceptional behavior of the **US1**– $H_2PO_4^-$ complex originates from the differences in the mode of solvation between this complex and others. The 2:2 complex, as reported in the solid state,⁹ as well as the 2:1 complex that was found in the nonpolar media,³² provides very good shielding of hydrophilic $H_2PO_4^-$ ions from the organic solutions. This peculiarity of phosphate ion binding manifests itself only in solution, and due to the lack of solvent interactions could not be detected in the gas phase. The importance of the entropic term in the anion complexation by uranyl salophenes in solution was pointed also by Rudkevich et al.,⁹ who found that enthalpic terms for the Cl^- and the $H_2PO_4^-$ complexes are comparable, while the observed stability constant of the $H_2PO_4^-$ complex was 37 times higher than that of the Cl^- complex. Shielding from the surrounding solvent (acetonitrile/DMSO, 99/1) could potentially also be a consequence of the tendency of the phosphate ions to dimerize. To the best of our knowledge, HSO_4^- ions do not form such stable dimers, which may prevent them from being effectively shielded from the solvent. This could explain the significant difference in the experimental binding affinities of $H_2PO_4^-$ and HSO_4^- to uranyl salophenes, despite their structural similarity.

Recently Coupez and Wipff³⁹ and Bruno et al.^{37b} stressed the crucial role of the solvent in the binding scheme of UO_2^{2+} ,

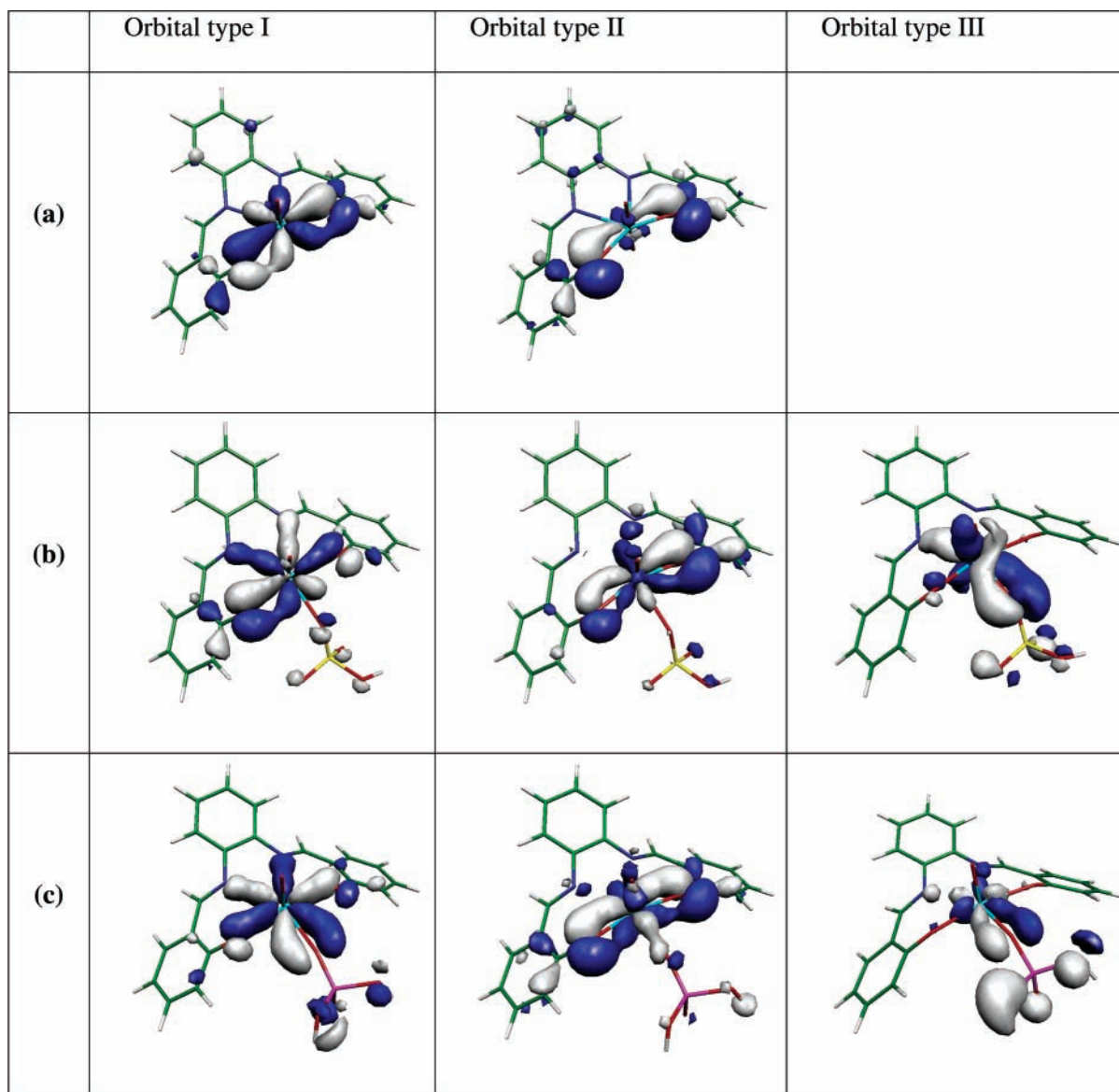


Figure 5. Selected molecular orbitals (MO) of US1 (a), and its anionic complexes: **US1–H₂PO₄[−]** (b), **US1–HSO₄[−]** (c).

TABLE 6: The Overlap Populations between Different Fragments in the Anionic Complexes of US1 Obtained from AOMix Program with KS(ECP) Method^a

MO	overlap	Anion					
		F [−]	Cl [−]	OH [−]	NO ₂ [−]	HSO ₄ [−]	H ₂ PO ₄ [−]
Type I	O ₁₂	0.041	0.021	0.047	0.020	0.032	0.030
	O ₁₃	0.0	0.002	0.001	0.0	−0.003	0.001
	O ₂₃	0.050	0.017	0.067	0.014	−0.001	0.026
Type II	O ₁₂	0.064	0.075	0.073	0.073	0.0055	0.056
	O ₁₃	0.0	0.004	0.0	0.001	−0.002	−0.001
	O ₂₃	−0.001	0.008	0.003	0.004	−0.013	−0.009
Type III	O ₁₂		0.0	−0.013	−0.012	0.002	0.005
	O ₁₃		0.0	0.001	−0.001	0.001	0.0
	O ₂₃		0.042	0.046	0.051	0.046	0.045

^a The subscripts for the overlapping fragments are: 1—salophene part, 2—uranyl cation, 3—anion (ex: O₂₃—overlap between the MO of the uranyl and the complexed anion).

showing that the gas-phase complexing properties differ significantly from those observed experimentally in the solution. Similarly, using an example of calix[4]pyrrole, Blas et al.^{16a} showed that the high affinity for F[−] in the gas phase might be lost in the presence of protic solvents, or the hydrated counterion.

Molecular Orbital Analysis of the Anionic Complexes.

Description of the bonding in the UO₂²⁺ ion found in the literature is somehow inhomogeneous, and many bonding schemes were proposed.⁴⁰ Nevertheless, the short U—O distances and the linearity of the ion suggest the presence of multiple bonding with a contribution from the 6p and 5f orbitals of the U atom. Different authors pointed out that the complexation and hydrolysis properties of UO₂²⁺ may indicate that the effective charge on the U atom in the complexes is higher than formal +2, and possibly exceeds +3, resulting in a strong polarization of the U—O bonds.⁴¹ Thus the total −2 charge supplied by the deprotonated salophene moiety may not fully compensate the effective charge of UO₂²⁺, leading to its strong affinity toward anions. To understand the relation between the electronic structure of the optimized complexes and their binding energies, we analyzed the distribution of the Mulliken charges (see Table 5 for KS(ECP) results, and Supporting Information for those of KS (ZORA)). The Mulliken charges using the KS(ZORA) and KS(ECP) methods show similar trends, but the differences in the charge distribution are less pronounced in the results from the former method. The presence of two

negatively charged phenoxyl groups in the salophene moiety significantly reduces the effective charge on the U atom with respect to bare UO_2^{2+} . The effective charge on the anion binding site remains, however, positive. The Mulliken charge on U is +1.25e. This result is in agreement with the high affinity of **US1** for anions and suggests strong contribution from the electrostatic interaction to the calculated binding energy.

Although the dominant role of the electrostatic term in the total energy of the complexes was underlined in most studies, some authors stressed the importance of the high electron affinity (15 eV) of the uranyl cation.³³ The *f* orbitals of UO_2^{2+} remain formally empty, and are good potential electron acceptors in the charge-transfer complexes. Comparison of data from Tables 3 and 5 shows that there is a direct correlation between the charge distribution and the binding energy in all **US1**–anion complexes. The decrease of the positive charge on the uranium atom is accompanied by an increase in the anion binding energy. The highest reduction of the charge on U is observed for the two most strongly bound ions (i.e., F^- and OH^-). The decrease of the positive charge on the U atom is accompanied by the increase of the negative charge on the axial oxygen atoms. Thus, part of the electron density donated to the U atom by an anion in the equatorial plane passes to the axial oxygen atoms of the uranyl moiety (Table 5).

No correlation was found between the binding energies and the charge distribution on the nitrogen or phenolic oxygen atoms. The latter is almost unaffected by the complexed ion, while the charge on the nitrogen is reduced for all the complexes from $-0.50e$ to about $-0.46e$. The effect is probably related to the increase of the UO_2 –N distance upon anion complexation. The U–N distance increases upon anion complexation by 0.162–0.216 Å, and no direct correlation between this elongation and binding energy can be seen (see Table 2). The negative charge of the *guest* molecule weakens the interaction with the free electron pairs of $\text{N}=\text{C}$ and moves the uranyl moiety out of the semi-cavity center.

The selected molecular orbitals of **US1** and its complexes with H_2PO_4^- and HSO_4^- ions are presented in Figure 5. The MOs for other complexes described in this paper can be found in the Supporting Information. The analysis of the electronic structure of the optimized complexes shows that the molecular orbitals involved in the bonding in different ionic complexes exhibit a rather complex shape. Nevertheless, some important information can be extracted from the shape and the characteristics of different molecular orbitals of the studied species. By detailed analysis of the shape of the MOs, their energy, and the overlap populations between the different fragments in the studied complexes, three characteristic types of bonding orbitals may be noticed. We label them as type I, II, and III. Type I is a hybrid bonding orbital with a major contribution from the $5f_{yz^2-x^2}$ orbital of uranium and an admixture of the *p* orbitals of O and N atoms of the salophene. Its shape reveals a noticeable electronic density between the uranyl moiety and surrounding oxygen and nitrogen atoms of the salophene. Types II and III are the bonding hybrid orbitals arising from the modified *5f* orbitals of uranium with a significant contribution from the salophene oxygen and the complexed anions, respectively.

The overlap populations of the above-mentioned three types of MOs composed of the three fragments are summarized in Table 6. For the sake of simplicity, in the following analysis of the molecular orbitals, the three components of the uranyl–salophene–anion complex orbitals are defined as follows: salophene part—“fragment 1”, the uranyl cation—“fragment 2”, and the complexed anion—“fragment 3”. A net correlation

between the overlap population O_{23} (overlap population between the uranyl cation and the complexed anion) for the MO type I (Figure 5 and Supporting Information) and the binding energy presented in Table 3 may be noticed. The increase in binding energy is always reflected in an increase of the overlap population between the uranyl center and the complexed anion. Although it is difficult to quantify this effect, the overall trends are well reproduced. Interestingly, the shape of the molecular orbital of type I in the complex of **US1** with the fluoride anion was found to be significantly distorted, which can be related to the fact that in this particular complex, an important perturbation of the molecular orbital occurs. Another interesting observation concerns the two most strongly bound ions (i.e., OH^- and F^-), for which the overlap populations between the uranyl cation and the salophene ligand (O_{12}) are clearly higher than in the remaining complexes, suggesting that the strong bonding character is also extended to the uranyl–salophene bonds.

Conclusions

Quantum chemistry calculations on the uranyl ion and its binary (uranyl salophene, **US1**) and ternary (uranyl salophene–anion, **US1**–anion) complexes, although complicated and time-consuming, due to the elevated number of electrons in the uranium atom, seem to be a promising tool in the elucidation of the electronic structure and thus the binding properties of the uranyl compounds. The calculated structure of **US1** agrees well with the X-ray geometry. Moreover, the calculated structures of the anionic (Cl^- and H_2PO_4^-) complexes of **US1** also show good agreement with the solid-state structures. Therefore, we believe that the structures of NO_2^- , F^- , HSO_4^- , and OH^- complexes, for which the experimental data are not available, provide a reasonable prediction. A good agreement between the experimental ^{13}C chemical shifts in the NMR spectrum and those calculated for the optimized geometry of **US1** suggests that the structure calculated in this work is also representative of that in the liquid phase.

For all studied anions, the KS(ZORA) and KS(ECP) anion binding energies calculated in the gas phase are very similar. Except for the phosphate ion, they correlate well with the experimental stability constants in solution. The highest values of binding energy were obtained for F^- and OH^- complexes. The noticeable discrepancy between the Gibbs free energy of complexation in solution and the gas-phase binding energy in the case of the H_2PO_4^- complexation stems probably from the solvent effects. In our opinion, the differences of solvation energies between free and complexed phosphate ions play a decisive role in understanding the thermochemistry of H_2PO_4^- complexation by **US1** in solution. In the structures proposed in the literature, the phosphate ions, either in monomeric or dimeric form, are surrounded by two molecules of the uranyl salophene. Due to such a shielding, the hydrophilic dihydrogenphosphate ion may be separated from the organic solvent. We postulate that this may provide an additional stabilization for the complex, reflected in the high value of the association constant for the **US1**– H_2PO_4^- complex in the condensed phase.

Acknowledgment. The authors thank the Swiss National Science Foundation for financial support. T.W. acknowledges the computer time grant from the Swiss Center for Scientific Computations in Manno. The work of M.B. at UC Davis was supported by Swiss National Science Foundation Grant 8220-067593.

Supporting Information Available: The geometries and Mulliken charges of free salophene and of uranyl salophene

(US1) complexes with anions optimized using KS(ZORA) method. Calculated ^{13}C chemical shifts with the corresponding shielding tensors. Molecular orbitals for uranyl–salophene complexes. The Cartesian coordinates for the optimized structures. Interaction energies without the BSSE correction. The X-ray structure of dioxo{2,2'-[1,2-phenylenebis(nitrilomethylidene)]-bis(6-methoxyphenolato)(2-)-*N,N',O,O'*]uranium- H_2PO_4^- .

References and Notes

- (1) Dacheux, N.; le Du, J. F.; Brandel, V.; Genet, M.; Decambox, P.; Moulin, C. *New J. Chem.* **1996**, *20*, 507.
- (2) Spalding, R. F.; Sackett, W. M. *Science* **1972**, *175*, 629.
- (3) Lamb, J. D.; Christensen, J. J.; Oscarson, J. L.; Nielsen, B. L.; Asay, B. W.; Izatt, R. M. *J. Am. Chem. Soc.* **1980**, *102*, 6820.
- (4) Thuéry, P.; Nierlich, M.; Masci, B.; Asfari, Z.; Vicens, J. *J. Chem. Soc., Dalton Trans.* **1999**, *18*, 3151.
- (5) Thuéry, P.; Nierlich, M.; Baldwin, B. W.; Komatzusaki, N.; Hirose, T. *J. Chem. Soc., Dalton Trans.* **1999**, *7*, 1047.
- (6) (a) Thuéry, P.; Keller, N.; Lance, M.; Vigner, J. D.; Nierlich, M. *New J. Chem.* **1995**, *19*, 619. (b) Sonoda, M.; Nishida, M.; Ishii, D.; Yoshida, I. *Anal. Sci.* **1999**, *15*, 1207.
- (7) Bandoli, G.; Clemente, D. A. *J. Chem. Soc., Dalton Trans.* **1975**, *7*, 612.
- (8) van Doorn, A. R.; Schaafstra, R.; Bos, M.; Harkema, S.; van Eerden, J.; Verboom, W.; Reinhoudt, D. N. *J. Org. Chem.* **1991**, *56*, 6083.
- (9) (a) Rudkevich, D. M.; Verboom, W.; Brzozka, Z.; Palys, M. J.; Stauthamer, W. P. R. V.; van Hummel, G. J.; Franken, S. M.; Harkema, S.; Engbersen, J. F. J.; Reinhoudt, D. N. *J. Am. Chem. Soc.* **1994**, *116*, 4341. (b) Rudkevich, D. M.; Stauthamer, W. P. R. V.; Verboom, W.; Engbersen, J. F. J.; Harkema, S.; Reinhoudt, D. N. *J. Am. Chem. Soc.* **1992**, *114*, 9671.
- (10) (a) Wroblewski, W.; Wojciechowski, K.; Dybko, A.; Brzozka, Z.; Egberink, R. J. M.; Snellink-Ruel, B. H. M.; Reinhoudt, D. N. *Sens. Actuators B* **2000**, *68*, 313. (b) Wroblewski, W.; Wojciechowski, K.; Dybko, A.; Brzozka, Z.; Egberink, R. J. M.; Snellink-Ruel, B. H. M.; Reinhoudt, D. N. *Anal. Chim. Acta* **2001**, *432*, 79.
- (11) Antonisse, M. M. G.; Snellink-Ruel, B. H. M.; Yigit, I.; Engbersen, J. F. J.; Reinhoudt, D. N. *J. Org. Chem.* **1997**, *62*, 9034.
- (12) Pepper, M.; Bursten, B. *Chem. Rev.* **1991**, *91*, 79.
- (13) Kaltsoyannis, N. *Chem. Soc. Rev.* **2003**, *32*, 9.
- (14) Pyykkö, P.; Li, J.; Runeberg, N. *J. Phys. Chem.* **1994**, *98*, 4809.
- (15) (a) Tsushima, S.; Yang, T.; Suzuki, A. *Chem. Phys. Lett.* **2001**, *334*, 365. (b) Tsushima, S.; Suzuki, A. *J. Mol. Struct. (THEOCHEM)* **1999**, *487*, 33. (c) Spencer, S.; Gagliardi, L.; Handy, N. C.; Ioannou, A. G.; Skylaris, C.-K.; Willetts, A. *J. Phys. Chem. A* **1999**, *103*, 1831.
- (16) (a) Schreckenbach, G. *Inorg. Chem.* **2002**, *41*, 6560. (b) Schreckenbach, G.; Wolff, S. K.; Ziegler, T. *J. Phys. Chem. A* **2000**, *104*, 8244.
- (17) (a) Craw, J. S.; Vincent, M. A.; Hillier, I. H.; Wallwork, A. L. *J. Phys. Chem.* **1995**, *99*, 10181. (b) Hutschka, F.; Dedieu, A.; Troxler, L.; Wipff, G. *J. Phys. Chem. A* **1998**, *102*, 3773. (c) Sémon, L.; Boehme, C.; Billard, I.; Hennig, C.; Lützenkirchen, K.; Reich, T.; Rosberg, A.; Rossini, I.; Wipff, G. *Chem. Phys. Phys. Chem.* **2001**, *2*, 591. (d) Tsushima, S.; Uchida, Y.; Reich, T. *Chem. Phys. Lett.* **2002**, *357*, 73. (e) Majumdar, D.; Balasubramanian, K.; Nitsche, H. *Chem. Phys. Lett.* **2002**, *361*, 143. (f) van Doorn, A. R.; Bos, M.; Harkema, S.; van Eerden, J.; Verboom, W.; Reinhoudt, D. N. *J. Org. Chem.* **1991**, *56*, 2371.
- (18) (a) Schreckenbach, G.; Hay, P. J.; Martin, R. L. *J. Comput. Chem.* **1999**, *20*, 70. (b) Schreckenbach, G.; Hay, P. J.; Martin, R. L. *Inorg. Chem.* **1998**, *38*, 4442.
- (19) (a) van Lenthe, E.; Baerends, E. J.; Snijders, J. G. *J. Chem. Phys.* **1994**, *101*, 9783. (b) van Lenthe, E.; Ehlers, A. E.; Baerends, E. J. *J. Chem. Phys.* **1999**, *110*, 8943.
- (20) (a) Fonseca Guerra, C.; Snijders, J. G.; te Velde, G.; Baerends, E. *J. Theor. Chem. Acc.* **1998**, *99*, 391. (b) ADF2002.03, SCM, Theoretical Chemistry, Vrije Universiteit, Amsterdam, The Netherlands, <http://www.scm.com>, Baerends, E. J.; Autschbach, J. A.; Bérces, A.; Bo, C.; Boerrigter, P. M.; Cavallo, L.; Chong, D. P.; Deng, L.; Dickson, R. M.; Ellis, D. E.; Fan, L.; Fischer, T. H.; Fonseca Guerra, C.; van Gisbergen, S. J. A.; Groeneveld, J. A.; Gritsenko, O. V.; Grüning, M.; Harris, F. E.; van den Hoek, P.; Jacobsen, H.; van Kessel, G.; Kootstra, F.; van Lenthe, E.; Osinga, V. P.; Patchkovskii, S.; Philipsen, P. H. T.; Post, D.; Pye, C. C.; Ravenek, W.; Ros, P.; Schipper, P. R. T.; Schreckenbach, G.; Snijders, J. G.; Sola, M.; Swart, M.; Swerhone, D.; te Velde, G.; Vernooijs, P.; Versluis, L.; Visser, O.; van Wezenbeek, E.; Wiesenekker, G.; Wolff, S. K.; Woo, T. K.; Ziegler, T. (c) Becke, A. D. *Phys. Rev. A* **1988**, *38*, 3098. (d) Perdew, J. P. *Phys. Rev. B* **1986**, *33*, 8822.
- (21) Frisch, M. J.; Trucks, G. W.; Schlegel, H. B.; Scuseria, G. E.; Robb, M. A.; Cheeseman, J. R.; Montgomery, J. A., Jr.; Vreven, T.; Kudin, K. N.; Burant, J. C.; Millam, J. M.; Iyengar, S. S.; Tomasi, J.; Barone, V.; Mennucci, B.; Cossi, M.; Scalmani, G.; Rega, N.; Petersson, G. A.; Nakatsuji, H.; Hada, M.; Ehara, M.; Toyota, K.; Fukuda, R.; Hasegawa, J.; Ishida, M.; Nakajima, T.; Honda, Y.; Kitao, O.; Nakai, H.; Klene, M.; Li, X.; Knox, J. E.; Hratchian, H. P.; Cross, J. B.; Adamo, C.; Jaramillo, J.; Gomperts, R.; Stratmann, R. E.; Yazyev, O.; Austin, A. J.; Cammi, R.; Pomelli, C.; Ochterski, J. W.; Ayala, P. Y.; Morokuma, K.; Voth, G. A.; Salvador, P.; Dannenberg, J. J.; Zakrzewski, V. G.; Dapprich, S.; Daniels, A. D.; Strain, M. C.; Farkas, O.; Malick, D. K.; Rabuck, A. D.; Raghavachari, K.; Foresman, J. B.; Ortiz, J. V.; Cui, Q.; Baboul, A. G.; Clifford, S.; Cioslowski, J.; Stefanov, B. B.; Liu, G.; Liashenko, A.; Piskorz, P.; Komaromi, I.; Martin, R. L.; Fox, D. J.; Keith, T.; Al-Laham, M. A.; Peng, C. Y.; Nanayakkara, A.; Challacombe, M.; Gill, P. M. W.; Johnson, B.; Chen, W.; Wong, M. W.; Gonzalez, C.; Pople, J. A. *Gaussian 03, Revision A.1*; Gaussian, Inc.: Pittsburgh, PA, 2003.
- (22) (a) Vetere, V.; Maldivi, P.; Adamo, C. *J. Comput. Chem.* **2003**, *24*, 850. (b) Vetere, V.; Maldivi, P.; Adamo, C. *Int. J. Quantum Chem.* **2003**, *91*, 321.
- (23) (a) Gorelsky, S. I.; Lever, A. B. P. *J. Organomet. Chem.* **2001**, *635*, 187. (b) Gorelsky, S. I.; AOMix program, Rev. 5.44. <http://www.obbligato.com/software/aomix/>.
- (24) (a) Kuechle, W.; Dolg, M.; Stoll, H.; Preuss, H. *J. Chem. Phys.* **1994**, *100*, 7535. (b) Kuechle, W.; Dolg, M.; Stoll, H. *J. Phys. Chem. A* **1997**, *101*, 7128. (c) Becke, A. D. *J. Chem. Phys.* **1993**, *98*, 5648. (d) Boys, S. F.; Bernardi, F. *Mol. Phys.* **1970**, *19*, 553.
- (25) Antonisse, M. M. G.; Snellink-Ruel, B. H. M.; Yigit, I.; Engbersen, J. F. J.; Reinhoudt, D. N. *Sens. Actuators B* **1998**, *47*, 9.
- (26) Merdivan, M.; Buchmeister, M. B.; Bonn, G. *Anal. Chim. Acta* **1999**, *402*, 91.
- (27) Stauthammer, W. Ph.D. Thesis, University of Twente, The Netherlands, 1994.
- (28) Wojciechowski, K.; Wroblewski, W.; Brzozka, Z. *Anal. Chem.* **2003**, *75*, 3270.
- (29) The barrier to rotation around the C(aromatic)–N bond in the protonated free salophene was estimated by calculating the energy of the ligand at fixed θ values (0 to 180° by 15°) and allowing the full relaxation of the remaining bonds and angles in the molecule. θ is the dihedral angle between the plane containing the phenylenediamine ring and the N=C bond. The calculations were performed using the KS(ECP) method.
- (30) Dalla Cort, A.; Madolini, L.; Palmieri, G.; Pasquini, C.; Schiaffino, L. *Chem. Commun.* **2003**, *17*, 2178.
- (31) Bagno, A.; Rastrelli, F.; Saielli, G. *J. Phys. Chem. A* **2003**, *107*, 9964.
- (32) Antonisse, M. M. G.; Snellink-Ruel, B. H. M.; Engbersen, J. F. J.; Reinhoudt, D. N. *J. Org. Chem.* **1998**, *63*, 9776.
- (33) Clavaguera-Sarrio, C.; Hoyou, S.; Ismail, N.; Marsden, C. J. *J. Phys. Chem. A* **2003**, *107*, 4515.
- (34) Evans, D. J.; Junk, P. C.; Smith, M. K. *Polyhedron* **2002**, *21*, 2421.
- (35) Tsushima, S.; Reich, T. *Chem. Phys. Lett.* **2001**, *347*, 127.
- (36) (a) Fuger, J.; Khodanovsky, I.; Sergeeva, E. J.; Medvedev, V. A.; Navrátil, J. D. In *The chemical thermodynamics of actinide elements and compounds, part 12. The actinide aqueous inorganic complexes*; IAEA: Vienna, 1992. (b) Alcock, N. W.; Esperas, S. J. *Chem. Soc., Dalton Trans.* **1977**, 893. (c) Howatson, J.; Grey, D. M.; Morosin, B. *J. Inorg. Nucl. Chem.* **1975**, *37*, 1929.
- (37) (a) Meinrath, G. *J. Radiat. Nucl. Chem.* **1997**, *224*, 119. (b) Vazquez, J.; Bo, C.; Poblet, J. M.; de Pablo, J.; Bruno, J. *Inorg. Chem.* **2003**, *42*, 6136.
- (38) Thatcher, G. R. J.; Cameron, D. R.; Nagelkerke, R.; Schmitke, J. *Chem. Soc., Chem. Commun.* **1992**, *4*, 386.
- (39) Coupez, B.; Wipff, G. *Inorg. Chem.* **2003**, *42*, 3693.
- (40) de Jong, W. A.; Visscher, L.; Nieuwpoort, W. C. *J. Mol. Struct. (THEOCHEM)* **1999**, *458*, 41.
- (41) See for example: (a) Connick, R. E.; Hugus, Z. Z., Jr. *J. Am. Chem. Soc.* **1952**, *74*, 6012. (b) Franczyk, T. S.; Czerwinski, K. R.; Raymond, K. N. *J. Am. Chem. Soc.* **1992**, *114*, 8138 and references therein.